Available online at www.sciencedirect.com
ScienceDirect
Trans. Nonferrous Met. Soc. China 32(2022) 3005−3014
Transactions of Nonferrous Metals Society of China
www.tnmsc.cn

PVDF−HFP binder for advanced zinc−manganese batteries

Shu-ci MA, Xiao-dong SHI, Zhe-xuan LIU, Yi-fan ZHOU, Pin-ji WANG, Jiang ZHOU, Shu-quan LIANG

Hunan Provincial Key Laboratory of Electronic Packaging and Advanced Functional Materials, School of Materials Science and Engineering, Central South University, Changsha 410083, China

Received 25 August 2021; accepted 25 December 2021

Abstract: In order to optimize and select the appropriate binder to improve the electrochemical performance of aqueous zinc−manganese batteries, the influences of water-soluble binders and oil-based binders on the zinc storage performance of manganese-based cathode materials were systematically investigated. The results show that the water-soluble binders with large numbers of hydroxyl and carboxyl groups are easily soluble in aqueous electrolytes, leading to poor electrochemical performance. Fortunately, the cathodes with polyvinylidene fluoride−hexafluoropropylene (PVDF−HFP) binder display high specific capacity of 264.9 mA·h/g and good capacity retention of 92% after 90 cycles at 100 mA/g. Meanwhile, PVDF−HFP binder with plenty of hydrophobic groups presents excellent ability in inhibiting cracks on the surface of electrode, reducing voltage polarization and charge transfer resistance, as well as maintaining electrode integrity.

Key words: aqueous zinc−manganese batteries; binders; PVDF−HFP; cycling stability

1 Introduction

The development of large-scale energy storage technology is the crux to the widespread use of renewable energy. In recent years, aqueous zinc−manganese batteries (ZMBs) have attracted wide attention because of their safety, environmentally friendly, high theoretical capacity of Zn anode (820 mA·h/g), etc [1−3]. At present, many modification strategies are devoted to improve the performance of aqueous ZMBs in terms of the cathode, anode and electrolyte [4−8]. However, there is little research on the binder of aqueous ZMBs. Although only a small amount of binder is used in electrode manufacturing, it plays a critical role in mechanical strength of electrodes and electrochemical performance of the batteries [9−11].

In aqueous ZMBs, polyvinylidene fluoride (PVDF) is commonly used binder on account of its chemical stability and insolubility in water. However, the active material cannot adapt to the huge volume change during cycle process due to the poor adhesion between the active material and the collector [12]. Water-soluble binders have been widely used in lithium-ion and sodium-ion batteries because of their low cost and non-pollution [13]. Sodium alginate (SA) contains a large number of carboxylic groups to provide good adhesion and less swelling in the electrolyte. The SA in the silicon anode makes the silicon particles have strong interaction and alleviate the volume expansion [14]. The introduction of SA and carboxyl methyl cellulose (CMC) binders in the phosphorous anodes of sodium-ion battery reduces the oxidation of activated phosphorus and maintains the structural integrity, which results in the excellent rate and cycling performance [15]. However, SA, CMC and other binders containing hydrophilic groups dissolve in water easily and can only be used in organic electrolytic cell. Therefore,

Corresponding author: Jiang ZHOU, E-mail: zhou_jiang@csu.edu.cn; Shu-quan LIANG, E-mail: lsq@csu.edu.cn
DOI: 10.1016/S1003-6326(22)65999-5

it is very important to develop suitable binders that can be used in aqueous ZMBs to promote the battery performance [16−18]. Polyvinylidene fluoride−hexafluoropropylene copolymer (PVDF−HFP) has been widely used as polymer matrix to form a gel electrolyte due to its good mechanical stability, low crystal characteristic, and high ionic conductivity [19−21]. CARDEA et al [22] used PVDF−HFP to prepare a membrane-like aerogel with highly hydrophobic nanosized pores and highly porous interconnected structure. SAITO et al [23] found that the interaction between the polymer and the electrolyte could affect the carrier concentration and fluidity of the gel electrolyte by adding PVDF−HFP. However, so far, there have been few relevant reports about PVDF−HFP as binder for aqueous ZMBs.

In this work, PVDF−HFP binder was firstly used in aqueous rechargeable ZMBs. We systematically studied the effects of water-soluble binders, e.g. SA, polytetrafluoroethylene (PTFE), carboxymethyl chitosan (CTS) and oily binders PVDF and PVDF−HFP on the electrochemical performance of aqueous ZMBs. This work may furnish new insight into the choice of binders for advanced ZMBs, which may promote their practical application.

2 Experimental

2.1 Material synthesis

SA, PTFE and CTS were dissolved in deionized water, while PVDF and PVDF−HFP are dissolved in NMP (N-methyl pyrrolidone, >99%, Sigma-Aldrich) solvent at room temperature. The preparation process of the $K_{0.27}MnO_2$ material was as follows: 5 mmol $KMnO_4$, 44 μL hydrofluoric acid and 30 mL deionized water were mixed and stirred for 0.5 h. After the solution was completely dissolved, the mixture was hydrothermally treated at 170 °C for 12 h. The prepared material was washed with deionized water, and then dried in a vacuum oven at 80 °C for 12 h.

2.2 Material characterization

X-ray diffraction (XRD) was performed on an X-ray diffractometer equipped with a Cu target X-ray tube in the 2θ range of 10°−80° at a scanning rate of 10 (°)/min. The morphology and microstructure of the as-prepared samples were examined via scanning electron microscopy (SEM; Hitachi SU8010).

2.3 Electrochemical measurement

In the electrode manufacturing process, a slurry was obtained by uniformly mixing 70 wt.% of the active material, 20 wt.% of conductive carbon, and 10 wt.% of the binder in a certain amount of solvent. The obtained slurry was evenly coated on the steel mesh and dried in a vacuum oven at 80 °C for 12 h. The diameter and mass loading of $K_{0.27}MnO_2$ electrode were 12 mm and 1−1.5 mg/cm^2, respectively. Then, the standard CR2016 coin-type battery was manufactured using the prepared electrode as the cathode, Zn foil (purity 99.99%) as the counter electrode, and a glass fiber as the separator. The electrolyte was composed of 2 mol/L $ZnSO_4$ and 0.1 mol/L $MnSO_4$. The galvanostatic current electrochemical measurement was performed on the LAND battery test system (LAND CT2001A, Wuhan, China) within the voltage range of 0.8−1.8 V. CHI 660D electrochemical workstation was used to test the cyclic voltammetry curve with a scan rate of 0.2 mV/s and a voltage range of 0.8−1.8 V and electrochemical impedance spectroscopy (EIS) was used at 0.01−10^5 Hz under the same current density.

3 Result and discussion

3.1 Physical and chemical performance of electrodes

The stability of the electrodes with different binders was tested. As shown in Fig. 1(a), in the water-soluble binder, the electrode with CTS binder produced tiny particles and the active material fell off from the collector. The active material of electrode surface with PTFE binder was only slightly peeled off, showing good stability. Surprisingly, the active material of the electrode with SA binder fell off seriously and the electrode with SA binder displayed the worst stability. This phenomenon indicated that water-soluble binders provided poor bonding ability. As presented in Fig. 1(b), this may be because the water-soluble binder contained many hydrophilic functional groups such as hydroxyl and carboxyl groups. The water-soluble binder easily formed hydrogen bonds with water and dissolved in water. The active material and conductive carbon cannot tightly

combine with the collector because of the poor bonding ability. Oily PVDF and PVDF−HFP binders were insoluble in water, so the electrodes displayed excellent integrality and stability. However, PVDF−HFP electrode exhibited better stability and integrity than PVDF electrode in water, which may be because PVDF−HFP binder contained more fluorine-containing functional groups [24,25].

Subsequently, the original morphology and wettability of the electrodes with different binders were further tested, as shown in Fig. 2. The wettability of the electrode could be expressed by the contact angle. The smaller the contact angle is,

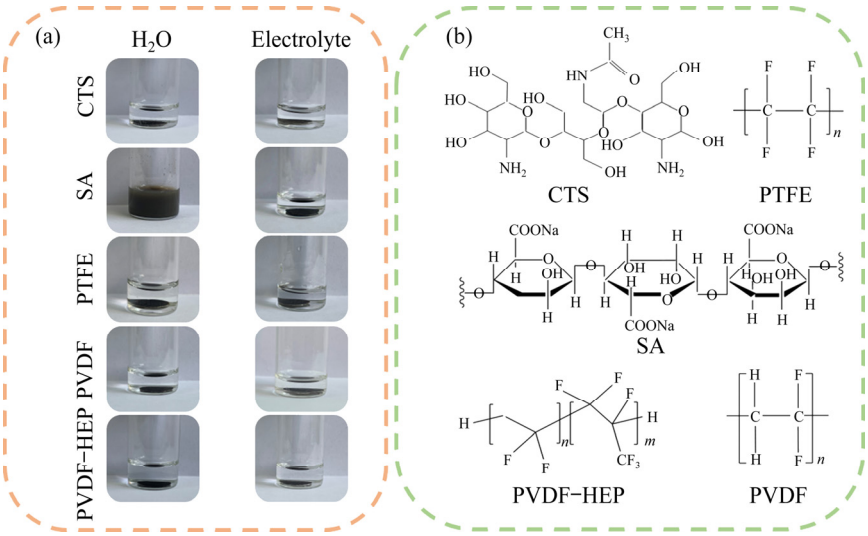

Fig. 1 Schematic diagrams showing stability test of electrodes with CTS, SA, PTFE, PVDF and PVDF−HFP binders soaked in water and electrolyte (2 mol/L $ZnSO_4$ + 0.1 mol/L $MnSO_4$) for 30 d, respectively (a), and chemical structures of CTS, SA, PTFE, PVDF, and PVDF−HFP binders (b)

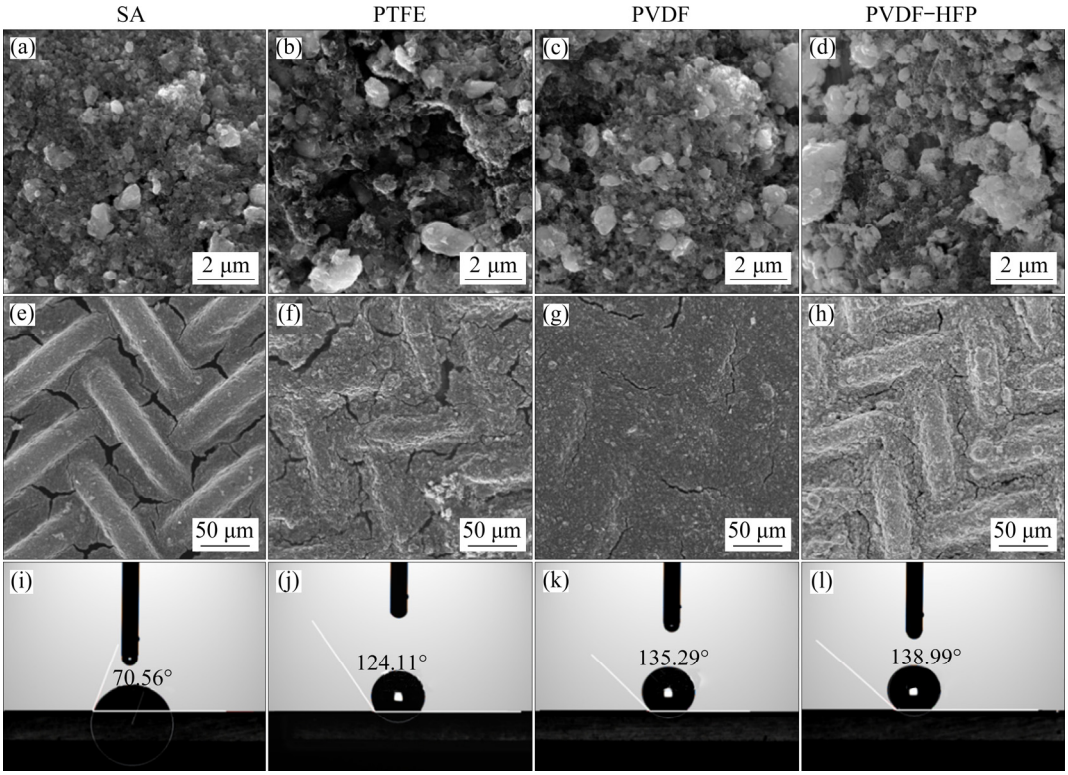

Fig. 2 SEM images of pristine electrodes with SA (a, e), PTFE (b, f), PVDF (c, g) and PVDF−HFP (d, h) binders, and contact angles of electrodes with SA (i), PTFE (j), PVDF (k) and PVDF−HFP (l) binders tested in 2 mol/L $ZnSO_4$ + 0.1 mol/L $MnSO_4$ electrolyte

the better the wettability of the electrode is. Wenzel equation is expressed as follows [26,27]:

$$\cos\theta^{*}=r\cos\theta$$

where θ^{*} is the rough surface contact angle, θ is the Young's contact angle on an ideal smooth surface, and r is roughness ratio. The larger the roughness is, the larger the contact angle is. When the contact angle was greater than 90°, the electrode surface exhibited hydrophobicity; while when the contact angle was less than 90°, the electrode surface exhibited hydrophilicity and was wetted with water. In Figs. 2(i–l) and Fig. S1 in Supporting Information, the contact angles of the electrodes with CTS, SA, PTFE, PVDF, and PVDF−HFP binders were 39.47°, 70.56°, 124.11°, 135.29° and 138.99°, respectively. The hydrophilicity of electrode with different binders from good to bad was CTS, SA, PTFE, PVDF and PVDF−HFP. The electrode with PVDF−HFP binder presented higher hydrophobicity than that with PVDF because of the introduction of fluorine-containing functional groups [28]. The water-soluble CTS, SA, and PTFE binders easily partly dissolved in excess water environment because of better hydrophilicity, which is consistent with the results in Fig. 1(a). This phenomenon also indicated that the water-soluble binders had poor bonding ability. Before cycle test, cracks of different sizes and degrees were produced on the surface of electrodes with water-soluble SA, PTFE and CTS binders, as shown in Figs. 2(a, b, e, f) and Fig. S2 in Supporting Information. The particles of electrode surface with PTFE binder agglomerated partially, and the surface cracks of electrode with PTFE binder were small. The surface cracks of electrode with SA binder were large and uniformly distributed. The surface cracks of electrode with CTS binder were the largest and widely distributed. Surprisingly, the particles of electrodes surface with oily PVDF and PVDF−HFP binders were evenly distributed. There were a few microcracks on the surface of electrode with PVDF binder and no cracks on the surface of electrode with PVDF−HFP binder.

3.2 Electrochemical performance of electrodes with different binders

To further understand the influence of binder on the electrochemical performance of cathode materials, the electrochemical behaviors and cyclic voltammetry (CV) curves of electrodes with different binders were compared, as shown in Fig. 3. The reduction peaks and oxidation peaks of electrodes with PVDF, PVDF−HFP and PTFE binders were located at 1.214/1.358, 1.232/1.367, 1.212/1.352 V and 1.613, 1.586, 1.634 V, respectively. However, one of the reduction peaks of electrodes with SA and CTS binders (Fig. S1 in Supporting Information) in Supporting Information) almost disappeared. The remaining reduction peaks and oxidation peaks were located at 1.232/1.359, 1.358/1.388 V and 1.656, 1.646 V, respectively, which indicated the polarization of electrodes with different binders from good to bad was PVDF−HFP, PVDF, PTFE, SA and CTS. The electrode with PVDF−HFP binder displayed the minimum polarization.

Meanwhile, as shown in Fig. 4, the initial discharge capacities of electrodes with water-soluble CTS (Fig. S1 in Supporting Information), SA, PTFE binders, oily PVDF and PVDF−HFP binders were 186, 259, 152, 273 and 248.7 mA·h/g, respectively. The initial coulombic efficiencies were 102.38%, 93.34%, 96.62%, 92.85% and 82.31%, respectively. The polarization phenomenon of electrodes with water-soluble binder was more and more serious during cycles. The capacity attenuation was obvious, which indicated the electrode material may have been damaged. Though the initial discharge capacity of electrode with PVDF−HFP binder was only 122 mA·h/g, as shown in Fig. 6(c), the capacity gradually increased and remained stable in subsequent cycles. The results also indicated that the electrode with PVDF−HFP binder displayed the minimum polarization and the best electron and ion transport dynamics during cycle process, which was consistent with the analysis in Fig. 3 [29].

The electrochemical impedance spectroscopy (EIS) reflected the interfacial resistance and ion diffusion of electrode materials. The spectrum was composed of two parts: the semicircle representing the medium and high frequency region and the straight line representing the low frequency range. A typical equivalent model (inset in Fig. 5(a)) and the impedance parameters for different electrodes (Table 1) were shown in Fig. 5, where R_0 is the ohmic resistance, CPE_1 represents the constant phase element, R_{ct} is the charge-transfer resistance,

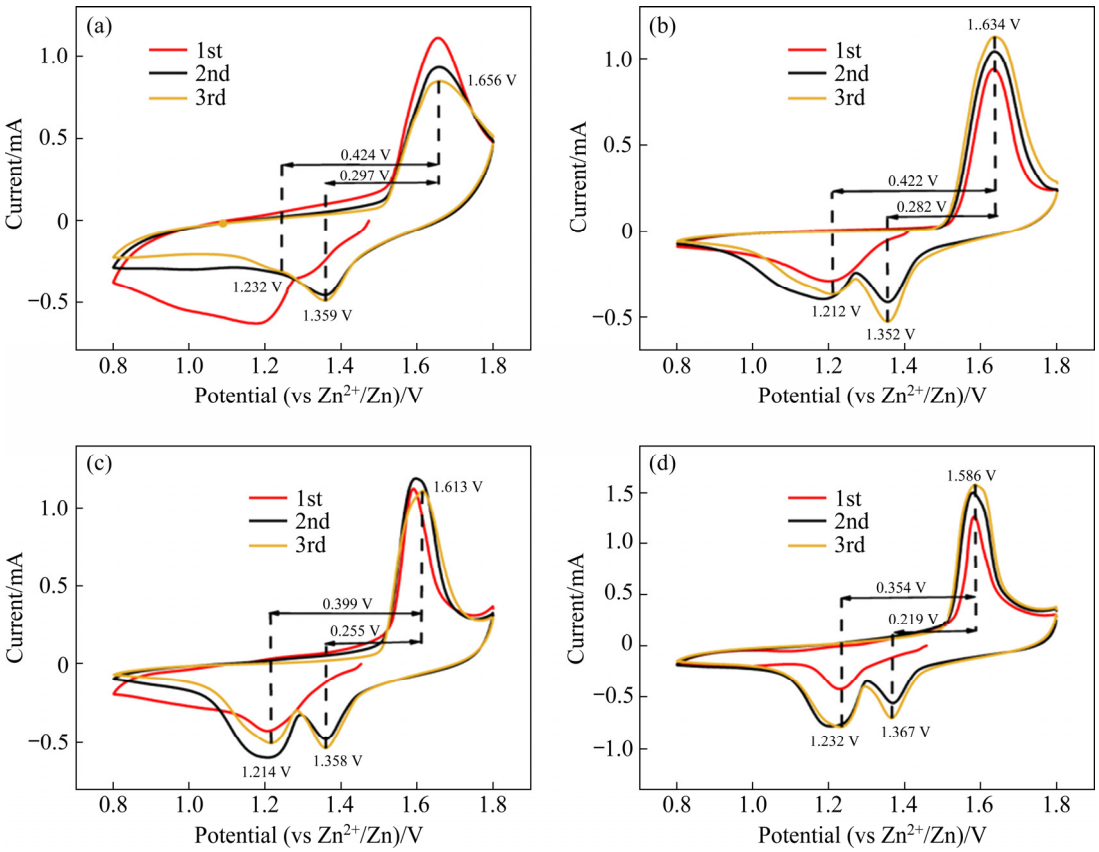

Fig. 3 CV curves of electrodes with SA (a), PTFE (b), PVDF (c) and PVDF−HFP (d) binders at 0.2 mV/s and 100 mA/g

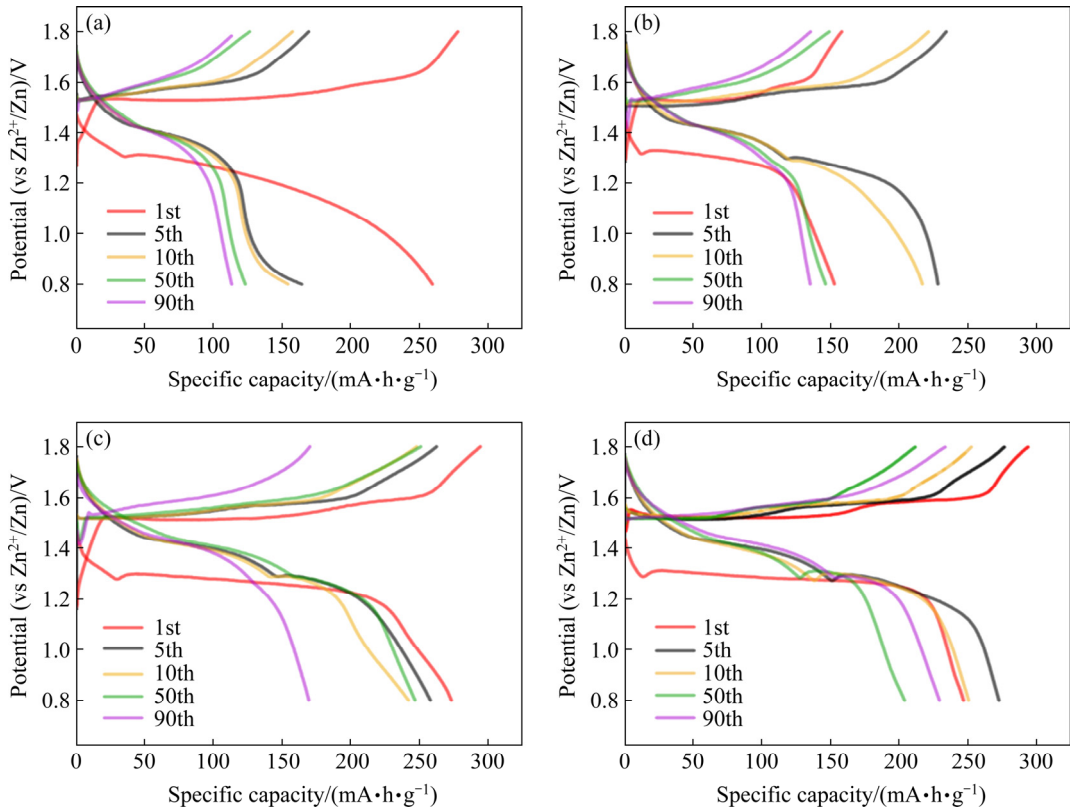

Fig. 4 Discharge−charge profiles of electrodes with SA (a), PTFE (b), PVDF (c) and PVDF−HFP (d) binders at 100 mA/g

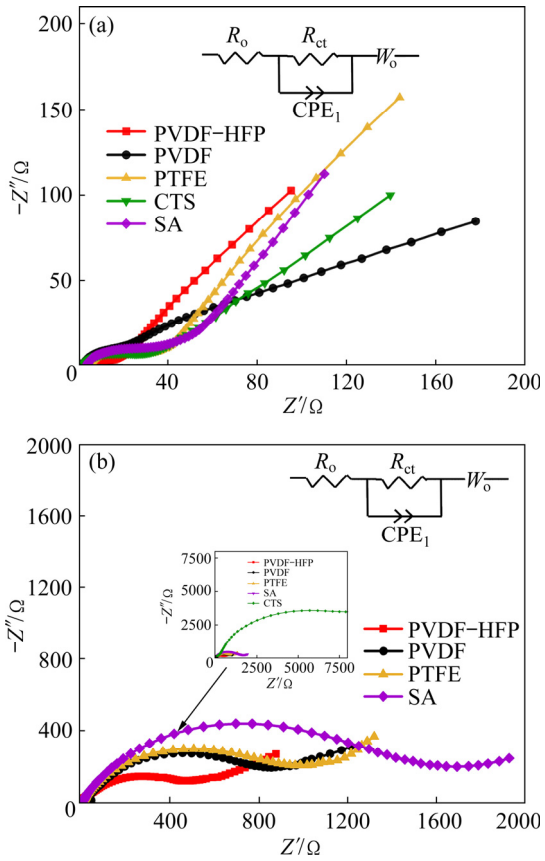

Fig. 5 Nyquist plots of electrodes with different binders before (a) and after (b) cycling at 500 mA/g

Table 1 Impedance parameters (R_{ct}) and ohmic resistance (R_o) of electrodes with different binders before and after cycles

Binder	R_{ct} before cycling/Ω	R_{ct} after cycling/Ω	R_o before cycling/Ω	R_o after cycling/Ω
PVDF−HFP	6.66	491.2	3.012	2.342
PVDF	11.67	735.3	1.61	38.88
PTFE	16.26	867.6	4.783	4.512
SA	17.53	1395	3.6	4.17
CTS	23.97	10548	2.54	2.7

and the inclined lines displayed in low frequency for different electrodes represent the Warburg impedance (W_o). Before cycling, the charge transfer resistances (R_{ct}) of electrodes with PVDF, PVDF−HFP, PTFE, SA and CTS binders were relatively low, which were 11.67, 6.66, 16.26, 17.53 and 23.97 Ω, respectively (Table 1). The electrode with PVDF−HFP binder displayed the minimum charge transfer resistance R_{ct}, which might be ascribed to good electron and ion mobility. After cycling, the charge transfer resistances R_{ct} of the electrodes with PVDF, PVDF−HFP, PTFE, SA and CTS binders increased, which were 735.3, 491.2, 867.6, 1395 and 10548 Ω, respectively (Table 1). The charge transfer resistance R_{ct} of the electrode with PVDF−HFP binder was much lower than that of other electrodes, which might be due to the introduction of the fluorine-containing functional groups and the smallest polarization during cycle process [30].

The cycling and rate performances of electrodes with different binders were evaluated and shown in Fig. 6. In Fig. 6(b), the electrode with PVDF−HFP binder displayed the highest specific capacity of 264.9 mA·h/g and capacity retention rate of 92% than that with other binders after 90 cycles. The water-soluble binder containing hydrophilic functional groups partially dissolved in excessive water and cannot provide strong bonding ability. The active material separated from the collector so that the electrode with water-soluble binders displayed poor electrochemical performance. The electrode with conventional PVDF binder demonstrated a capacity retention rate of only 61%, much lower than that of the electrode with PVDF−HFP binder. This is because the electrode with PVDF−HFP binder containing large numbers of fluorine-containing functional groups changed the hydrophobicity of electrode, which prevented the electrolyte from penetrating and destroying the electrode. In Figs. 6(a) and (c), the rate capability and long cycle performance of electrodes with different binders were compared. Since the cycle performance of electrodes with water-soluble binder was particularly poor at high current density, the long cycle performance of electrodes with PVDF and PVDF−HFP binders was mainly shown (Fig. 6(c)). The experimental data showed that the electrode with PVDF−HFP binder displayed the high capacity and excellent cycle performance.

3.3 Structure evolution of electrodes with different binders

The SEM images and the schematic diagram of structure evolution of electrodes with different binders after cycling were displayed, as shown in Fig. 7, and more microcracks of the electrode with PVDF binder were observed after cycling. Though only a few particles of the electrode with PVDF

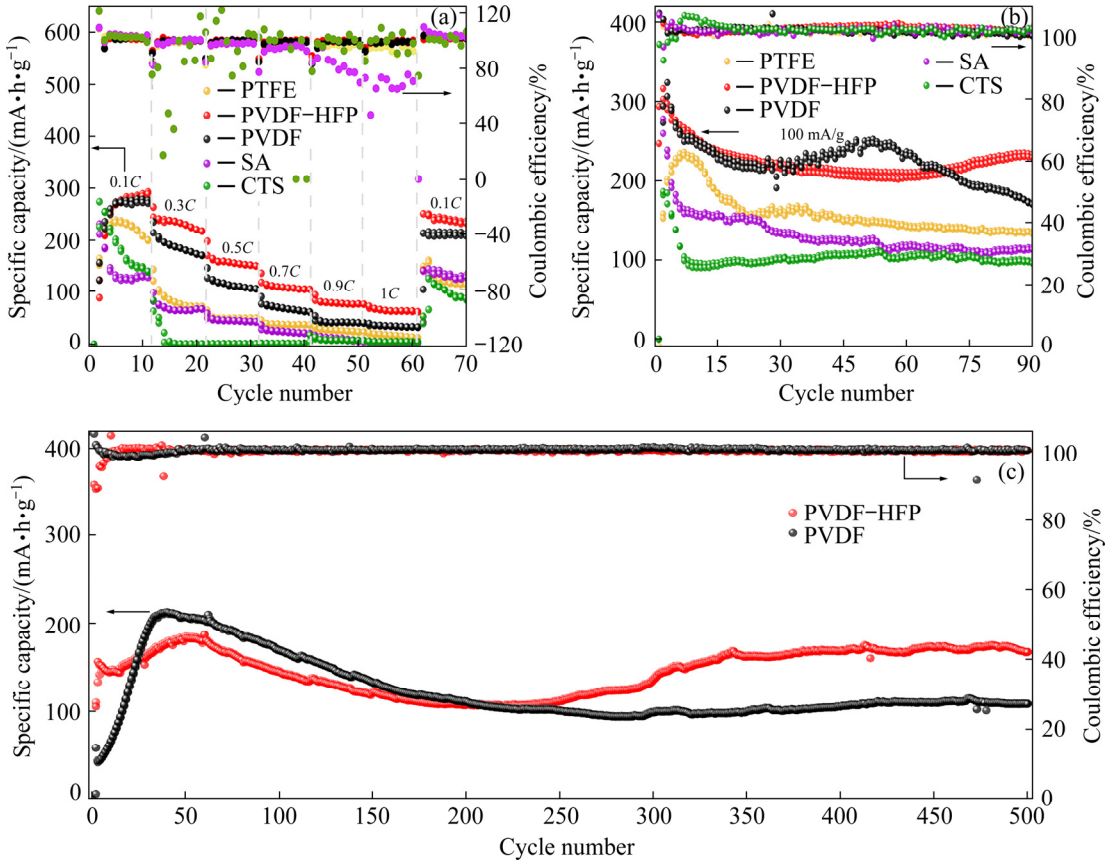

Fig. 6 Rate capability (a) and cycling performance (b) of electrodes with different binders at 100 mA/g and long cycling performance of electrodes with PVDF−HFP and PVDF binders at 500 mA/g (c)

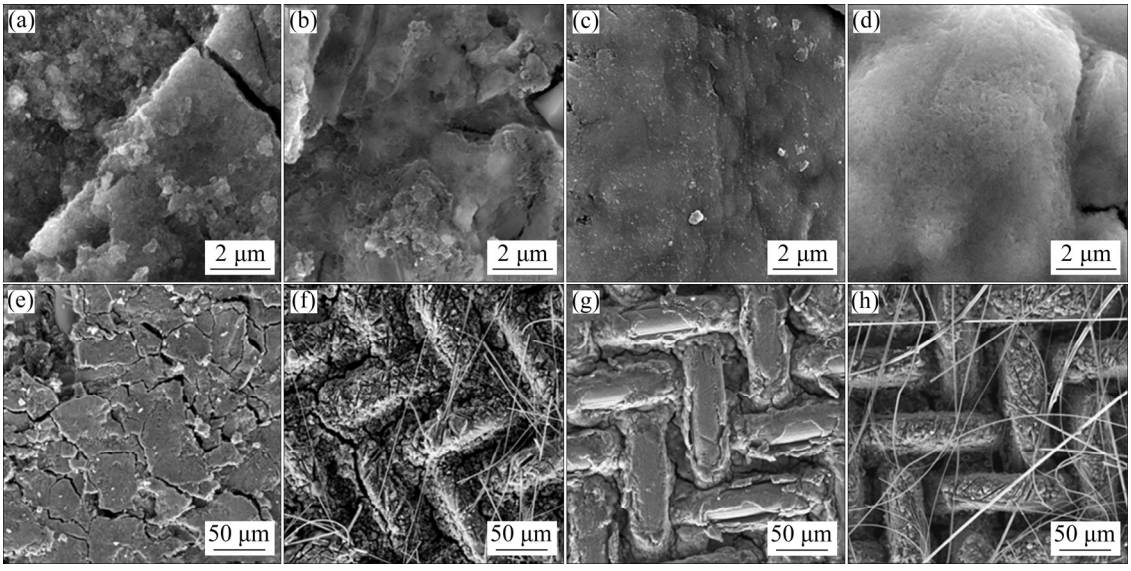

Fig. 7 SEM images of electrodes with SA (a, e), PTFE (b, f), PVDF (c, g) and PVDF−HFP (d, h) binders after 90 cycles

binder shed and destroyed, the integrity of the electrode was still maintained. Meanwhile, there were no microcracks on the surface of electrode with PVDF−HFP binder. This phenomenon may be due to the formation of many microporous structures on the surface of electrode, alleviating the volume expansion of the active material during cycling.

As shown in Fig. 8, the particles of the electrode with PVDF−HFP binder were combined

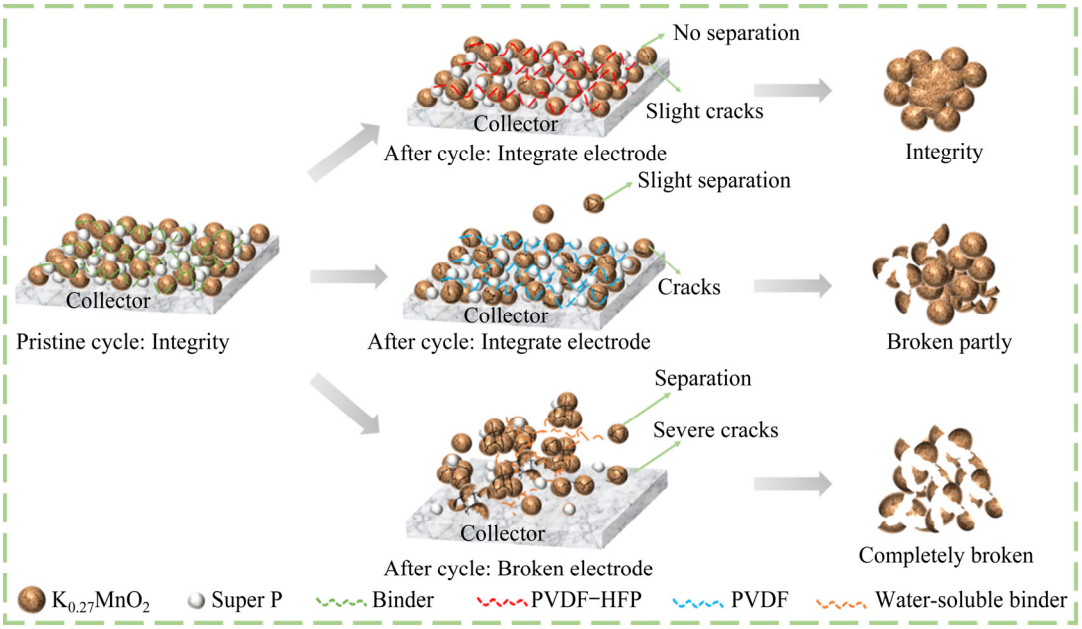

Fig. 8 Schematic diagram of structure evolution for electrodes with PVDF−HFP, PVDF and water-soluble binders

strongly and did not separate from the collector although the surface of particles displayed a few slight cracks. The electrode with PVDF−HFP binder maintained better integrity and displayed minimum polarization during cycling, thus displaying excellent electrochemical performance, which were consistent with the results in Fig. 3 and Fig. 6(b). Meanwhile, the particles of the electrode with PVDF binder slightly separated from the collector and the surface of particles displayed cracks, so that the electrode with PVDF binder broke partly. However, more cracks of electrode with CTS (Fig. S1 in Supporting Information) and SA binders were observed. The particles of electrode with CTS binder were locally aggregated. The electrode with SA binder was damaged and formed many fragments. The cracks of electrode surface with PTFE binder were less and larger (Figs. 7(e) and (f)). As shown in Fig. 8, the water-soluble binder provided poor bonding capability so that many active material particles severely separated from the collector and displayed severe cracks. The integrity of electrode with water-soluble binder was severely destroyed, which resulted in poor electrochemical performance (Fig. 8).

4 Conclusions

(1) Water-soluble binders were significantly inferior to oily binders, because water-soluble binders contained large numbers of hydrophilic functional groups. In the excessive water environment, the water-soluble binders were easy to partially dissolve in the electrolyte, resulting in poor bonding ability, which made the active material easily break away from the collector.

(2) Compared with the traditional PVDF binder, the introduction of fluorine-containing functional groups on PVDF−HFP binder could improve the hydrophobicity of the electrode. Compared with the capacity retentions of 61%, 52% and 44% for PVDF, CTS and SA electrodes, respectively, the PVDF−HFP electrode displayed a higher discharge capacity of 264.9 mA·h/g and a superior capacity retention of 92% after 90 cycles at 100 mA/g.

(3) PVDF−HFP binder displayed an important role in the suppression of electrode surface cracks, separated the active material from the collector, and maintained the integrity of the electrode. Meanwhile, it also reduced the charge transfer resistance and polarization, and significantly improved the electrochemical performance.

Supporting Information

Supporting Information is available at http://www.ysxbcn.com/download/16-p3005-supporting_information.pdf

Acknowledgments

This work was supported by the National Natural Science Foundation of China (Nos.

51932011, 51972346), the Hunan Natural Science Fund for Distinguished Young Scholar, China (No. 2021JJ10064), the Program of Youth Talent Support for Hunan Province, China (No. 2020RC3011), and the Innovation-Driven Project of Central South University, China (No. 2020CX024).

References

[1] ZHOU Shi-hao, WU Xian-wen, XIANG Yan-hong, ZHU Ling, LIU Zhi-xiong, ZHAO Cai-xian. Manganese-based cathode materials for aqueous zinc ion batteries [J]. Progress in Chemistry, 2021, 33: 649−669.

[2] SONG Ming, TAN Hua, CHAO Dong-liang, FAN Hong-jin. Recent advances in Zn-ion batteries [J]. Advanced Functional Materials, 2018, 28: 1802564.

[3] WU Xian-wen, LONG Feng-ni, XIANG Yan-hong, JIANG Jian-bo, WU Jian-hua, XIONG Li-zhi, ZHANG Qiao-bao. Research progress of anode materials for zinc-based aqueous battery in a neutral or weak acid system [J]. Progress in Chemistry, 2021, 33(11): 1983−2001.

[4] HAO Jun-nan, LI Xiao-long, ZENG Xiao-hui, LI Dan, MAO Jian-feng, GUO Zai-ping. Deeply understanding the Zn anode behaviour and corresponding improvement strategies in different aqueous Zn-based batteries [J]. Energy & Environmental Science, 2020, 13: 3917−3949.

[5] WANG Pin-ji, XIE Xue-song, XING Zhen-yue, CHEN Xian-hong, FANG Guo-zhao, LU Bing-an, ZHOU Jiang, LIANG Shu-quan, FAN Hong-jin. Mechanistic insights of Mg^{2+}-electrolyte additive for high-energy and long-life zinc-ion hybrid capacitors [J]. Advanced Energy Materials, 2021, 11: 2101158.

[6] ZHANG Teng-sheng, TANG Yan, FANG Guo-zhao, ZHANG Chen-yang, ZHANG Hong-liang, GUO Xun, CAO Xin-xin, ZHOU Jiang, PAN An-qiang, LIANG Shu-quan. Electrochemical activation of manganese-based cathode in aqueous zinc-ion electrolyte [J]. Advanced Functional Materials, 2020, 30: 2002711.

[7] SADAWY M, SAAD S, ABDEL-KARIM R. Effect of Zn/Mg ratio on cathodic protection of carbon steel using Al−Zn−Mg sacrificial anodes [J]. Transactions of Nonferrous Metals Society of China, 2020, 30: 2067−2078.

[8] PENG Ke, ZHANG Zhi-jian, ZHAO Ze-jun, YANG Chao, TIAN Zhong-liang, LAI Yan-qing. Performance of carbon-coated nano-ZnO prepared by carbonizing gel precursor as anodic material for secondary alkaline Zn batteries [J]. Transactions of Nonferrous Metals Society of China, 2019, 29: 2151−2159.

[9] ZHANG Tao, LI Jun-tao, LIU Jie, DENG Ya-ping, WU Zhen-guo, YIN Zu-wei, GUO Dong, HUANG Ling, SUN Shi-gang. Suppressing the voltage-fading of layered lithium-rich cathode materials via an aqueous binder for Li-ion batteries [J]. Chemical Communications, 2016, 52: 4683−4686.

[10] ZHAO Jing, YANG Xu, YAO Ye, GAO Yu, SUI Yong-ming, ZOU Bo, EHRENBERG H, CHEN Gang, DU Fei. Moving to aqueous binder: A valid approach to achieving high-rate capability and long-term durability for sodium-ion battery [J]. Advanced Science, 2018, 5: 1700768.

[11] HUANG Ying-yi, SHAIBANI M, GAMOT T D, WANG Ming-chao, JOVANOVIĆ P, COORAY M C D, MIRSHEKARLOO M S, MULDER R J, MEDHEKAR N V, HILL M R, MAJUMDER M. A saccharide-based binder for efficient polysulfide regulations in Li−S batteries [J]. Nature Communications, 2021, 12: 5375.

[12] CHANG H J, RODRÍGUEZ-PÉREZ I A, FAYETTE M, CANFIELD N L, PAN Hui-lin, CHOI D, LI Xiao-lin, REED D. Effects of water-based binders on electrochemical performance of manganese dioxide cathode in mild aqueous zinc batteries [J]. Carbon Energy, 2021, 3: 473−481.

[13] XU Hang, JIANG Ke-zhu, ZHANG Xue-ping, ZHANG Xiao-yu, GUO Shao-hua, ZHOU Hao-shen. Sodium alginate enabled advanced layered manganese-based cathode for sodium-ion batteries [J]. ACS Applied Materials & Interfaces, 2019, 11: 26817−26823.

[14] KANG K, LEE H S, HAN D W, KIM G S, LEE D H, LEE G, KANG Y M, JO M H. Maximum Li storage in Si nanowires for the high capacity three-dimensional Li-ion battery [J]. Applied Physics Letters, 2010, 96: 053110.

[15] XIAO Wei, SUN Qian, BANIS M N, WANG Bi-qiong, LI Wei-han, Li Min-si, LUSHINGTON A, Li Ru-ying, LI Xi-fei, SHAM T K, SUN Xue-liang. Understanding the critical role of binders in phosphorus/carbon anode for sodium-ion batteries through unexpected mechanism [J]. Advanced Functional Materials, 2020, 30: 2000060.

[16] WU Zhan-yu, DENG Li, LI Jun-tao, HUANG Qi-sen, LU Yan-qiu, LIU Jie, ZHANG Tao, HUANG Ling, SUN Shi-gang. Multiple hydrogel alginate binders for Si anodes of lithium-ion battery [J]. Electrochimica Acta, 2017, 245: 363−370.

[17] PATRA J, RATH P C, LI C, KAO H M, WANG F M, LI J, CHANG J K. A water-soluble NaCMC/NaPAA binder for exceptional improvement of sodium-ion batteries with an SnO_2-ordered mesoporous carbon anode [J]. ChemSusChem, 2018, 11: 3923−3931.

[18] LING Li-ming, BAI Ying, WANG Zhao-hua, NI Qiao, CHEN Guang-hai, ZHOU Zhi-ming, WU Chu-an. Remarkable effect of sodium alginate aqueous binder on anatase TiO_2 as high-performance anode in sodium ion batteries [J]. ACS Applied Materials & Interfaces, 2018, 10: 5560−5568.

[19] YEON S H, KIM K S, CHOI S, CHA J H, LEE H. Characterization of PVdF(HFP) gel electrolytes based on 1-(2-hydroxyethyl)-3-methyl imidazolium ionic liquids [J]. Journal of Physical Chemistry B, 2005, 109: 17928−17935.

[20] SAWANE Y B, OGALE S B, BANPURKAR A G. Low voltage electrowetting on ferroelectric PVDF−HFP insulator with highly tunable contact angle range [J]. ACS Applied Materials & Interfaces, 2016, 8: 24049−24056.

[21] YI Qiang, ZHANG Wen-qiang, LI Shao-qing, LI Xin-yuan, SUN Chun-wen. Durable sodium battery with a flexible $Na_3Zr_2Si_2PO_{12}$−PVDF−HFP composite electrolyte and sodium/carbon cloth anode [J]. ACS Applied Materials & Interfaces, 2018, 10: 35039−35046.

[22] CARDEA S, GUGLIUZZA A, SESSA M, ACETO M C,

DRIOLI E, REVERCHON E. Supercritical gel drying: A powerful tool for tailoring symmetric porous PVDF−HFP membranes [J]. ACS Applied Materials & Interfaces, 2009, 1: 171−180.

[23] SAITO Y, KATAOKA H, CAPIGLIA C, YAMAMOTO H. Ionic conduction properties of PVDF−HFP type gel polymer electrolytes with lithium imide salts [J]. Journal of Physical Chemistry B, 2000, 104: 2189−2192.

[24] DING Yang-yang, ZHONG Xin, YUAN Chun-mei, DUAN Lian-feng, ZHANG Long, WANG Zhe, WANG Chun-sheng, SHI Feng-wei. Sodium alginate binders for bivalency aqueous batteries [J]. ACS Applied Materials & Interfaces, 2021, 13: 20681−20688.

[25] SENTHIL R A, THEERTHAGIRI J, MADHAVAN J. Optimization of performance characteristics of 2-mercaptopyridine-doped polyvinylidene fluoride (PVDF) polymer electrolytes for dye-sensitized solar cells [J]. Journal of Non-Crystalline Solids, 2014, 406: 133−138.

[26] BATCHELOR T, CUNDER J, FADEEV A Y. Wetting study of imidazolium ionic liquids [J]. Journal of Colloid and Interface Science, 2009, 330: 415−420.

[27] ISAKOV K, KAUPPINEN C, FRANSSILA S, LIPSANEN H. Super-hydrophobic antireflection coating on glass using grass-like alumina and fluoropolymer [J]. ACS Applied Materials & Interfaces, 2020, 12: 49957−49962.

[28] JAIKRAJANG N, KAO-IAN W, MURAMATSU T, CHANAJAREE R, YONEZAWA T, AL BALUSHI Z Y, KHEAWHOM S, CHEACHAROEN R. Impact of binder functional groups on controlling chemical reactions to improve stability of rechargeable zinc-ion batteries [J]. ACS Applied Energy Materials, 2021, 4: 7138−7147.

[29] CHEN Wei, QIAN Tao, XIONG Jie, XU Na, LIU Xue-jun, LIU Jie, ZHOU Jin-qiu, SHEN Xiao-wei, YANG Ting-zhou, CHEN Yu, YAN Cheng-lin. A new type of multifunctional polar binder: Toward practical application of high energy lithium sulfur batteries [J]. Advanced Materials, 2017, 29: 1605160.

[30] MU Peng-zhou, ZHANG Huan-rui, JIANG Hong-zhu, DONG Tian-tian, ZHANG Shu, WANG Chen, LI Jie-dong, MA Yue, DONG Shan-mu, CUI Guang-lei. Bioinspired antiaging binder additive addressing the challenge of chemical degradation of electrolyte at cathode/electrolyte interphase [J]. Journal of the American Chemical Society, 2021, 143: 18041−18051.

PVDF−HFP 黏结剂用于高性能锌锰电池

马书辞，史晓东，刘哲轩，周一帆，王品基，周 江，梁叔全

中南大学 材料科学与工程学院 电子封装与先进功能材料湖南省重点实验室，长沙 410083

摘 要：为了优化和选择合适的黏结剂提高水系锌锰电池的电化学性能，系统地研究水溶性黏结剂和油性黏结剂对锰基正极材料储锌性能的影响。结果表明，含有大量羟基和羧基官能团的水溶性黏结剂易溶于水系电解液，导致较差的电化学性能。幸运的是，采用聚偏氟乙烯−六氟丙烯(PVDF−HFP)黏结剂制备的正极材料在电流密度为 100 mA/g 下循环 90 周后表现出 264.9 mA·h/g 的高比容量，容量保持率达到 92%。与此同时，含有大量疏水性官能团的 PVDF−HFP 黏结剂在抑制电极表面裂纹、降低电压极化和电荷转移电阻、保持电极完整性方面表现出优异的能力。

关键词：水系锌锰电池；黏结剂；PVDF−HFP；循环稳定性

(Edited by Wei-ping CHEN)